Journal of The Electrochemical Society, **150** (2) C61-C66 (2003)
0013-4651/2002/150(2)/C61/6/$7.00 © The Electrochemical Society, Inc.

Superconformal Electrodeposition of Silver from a $KAg(CN)_2$-KCN-KSeCN Electrolyte

B. C. Baker,[a,*] M. Freeman,[b] B. Melnick,[b] D. Wheeler,[a] D. Josell,[a,z] and T. P. Moffat[a,*]

[a]*National Institute of Standards and Technology, Gaithersburg, Maryland 20899, USA*
[b]*Motorola, Advanced Product Research and Development Laboratory, Austin, Texas 78721, USA*

Electrodeposition of silver from a $KAg(CN)_2$-KCN electrolyte was investigated. The addition of potassium selenocyanate (KSeCN) results in a hysteretic current-voltage response, specular films, and superconformal growth in submicrometer vias. These observations are well described by the recently proposed curvature enhanced accelerator coverage model of film growth.
 [DOI: 10.1149/1.1531195]

Manuscript submitted May 28, 2002; revised manuscript received July 19, 2002. Available electronically December 23, 2002.

The success of copper electrodeposition for interconnect metallization has spurred interest in the potential application of silver which has an even higher electrical conductivity and thus the promise of a lower resistance-capacitance circuit time constant.[1] To be a viable alternative, the silver films must also exhibit comparable or superior resistance to electromigration[2,3] and the deposition process must be capable of void or seam-free filling of submicrometer features. Recently, a commercial silver cyanide plating solution was shown to be capable of filling submicrometer trenches[4] and vias.[5] The results were described by the curvature-enhanced accelerator coverage (CEAC) model which successfully explained superconformal electrodeposition of copper[6-8] and silver[4,5] and chemical vapor deposition (CVD) of copper.[9] The essence of the CEAC model is that (*i*) the local deposition rate is determined by the coverage of a catalytic surface species and (*ii*) the local coverage changes in response to the changing area (therefore curvature) of the growth front. Thus, the diminishing area associated with growth at the bottom of a trench or via results in an increase in catalyst coverage and an accelerated metal deposition rate which gives rise to ''bottom-up'' or superconformal deposition. In the case of silver plating, selenium was identified as the catalytic surface species because its coverage scaled with rising current-time (chronoamperometric) transients. A significant limitation of the early silver work was incomplete knowledge of the electrolyte constituents, *i.e.*, the nature of the catalyst precursor and the influence of additional surfactants. The unknown composition (constituents) of the electrolyte prevented deeper understanding of the silver deposition process, hindering further development for superconformal filling processes.

In this paper, a silver cyanide electrolyte is fully disclosed which enables a more precise assessment of the CEAC model as it relates to this new class of ''superfilling'' electrolytes relevant to new industrial silver processes.[10]

Experimental

Silver cyanide solutions consisted of 0.34 mol/L $KAg(CN)_2$ and 2.3 mol/L KCN. Selenium was added as KSeCN and diluted from a 200 μmol/L KSeCN solution in the matrix shown above to concentrations between 0.02 and 20 μmol/L.

Electrochemical data was obtained on a planar silver electrode in solutions with no agitation at room temperature (~23°C). The silver cathode was polished with 320 SiC paper, rinsed with distilled water, and dried with N_2 prior to each deposition run. The masked area for deposition was 0.97 cm^2. A silver (99.99%) rod, polished and rinsed between experiments, was used as a reference electrode, while a Pt anode was situated coplanar with the working electrode. Experiments were done in a cell containing 100 mL of electrolyte into which aliquots of KSeCN solution were added. A sweep rate of 1 mV/s was used when cycling voltage.

Studies of feature filling in the silver cyanide electrolytes took place in the same setup used for the studies with planar substrates. A silver plated clip was used to contact scribed wafer pieces. Wafers, patterned with vias of a wide range of spacing and diameter, with a 100 nm copper seed, were used. Samples were plated potentiostatically *vs.* the Ag reference electrode. The stability of the electrolytes was tested by ensuring that current-voltage i-η curves in the solution at the beginning and end of each set of experiments were reproducible. After plating, the specimens were covered in epoxy and a glass coverslip and cross sectioned. Polishing was accomplished using diamond lapping films down to 0.1 μm grit followed by Ar^+ ion polishing at 13° from the plane of the specimen.

Results

Electrochemical.—The i-η curve for the $KAg(CN)_2$-KCN solution is shown in Fig. 1a. Slight hysteresis is apparent, with smaller current on the returning sweep. In sharp contrast, additions of KSeCN result in marked hysteresis of the i-η curves whereby the current is substantially increased on the return sweeps (Fig. 1a and b). The hysteresis is significant even at a concentration of only 0.2 μmol/L. The resulting deposits were also visibly brighter than those deposited in the absence of the catalyst. The hysteretic behavior results from cumulative adsorption of $SeCN^-$ catalyst on the metal surface occurring on the same time scale as the voltage sweep. The minimal hysteresis between the negative and reverse potential sweeps for the 19.4 μmol/L electrolyte indicates that saturation of the catalyst coverage occurs rapidly at this higher concentration in the electrolyte. The deposits at this concentration are not optically bright, unlike specimens deposited at the lower concentrations. This occurs despite the significantly shorter duration exposure to the destabilizing silver concentration gradient (*i.e.*, swept to only −0.4 V compared to −0.6 V for 4.9 μmol/L i-η curve). This is an expected consequence of the CEAC mechanism for a saturated surface. Acceleration of deposition rate in chronoamperometric the experiments due to the gradual adsorption of the catalyst, is also as expected (Fig. 2).

Simulations.—The CEAC mechanism was used to describe the electrochemical data presented above. A summary of the relevant equations is shown below

$$i(\theta, \eta) = i_o(\theta)\frac{C^i_{Ag}}{C_{Ag}}\left[\exp\left(-\frac{\alpha(\theta)F}{RT}\eta\right) - \exp\left(\frac{[1-\alpha(\theta)]F}{RT}\eta\right)\right] \quad [1]$$

* Electrochemical Society Active Member.
z E-mail: daniel.josell@nist.gov

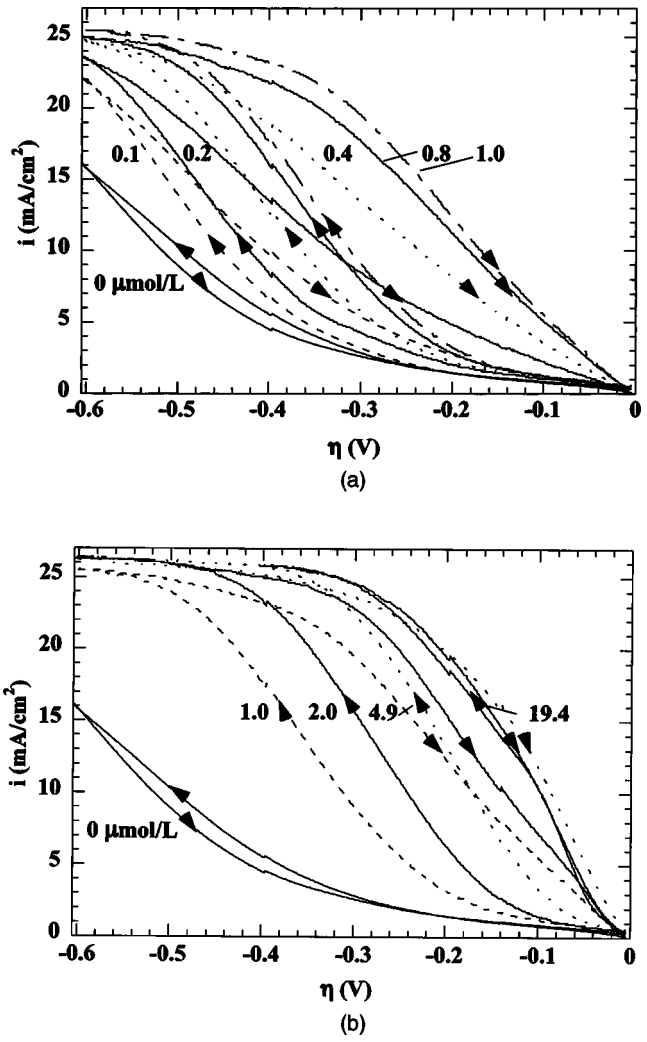

Figure 1. Effect of KSeCN concentration on the i-η response in electrolyte containing 0.34 mol/L $KAg(CN)_2$, 2.3 mol/L KCN, and (a) 0 to 1 μM KSeCN and (b) 1 to 19.4 μmol/L KSeCN.

$$\frac{d\theta}{dt} = \frac{i\Omega_{Ag}}{F}\kappa\theta + kC^{i}_{Se}(1 - \theta) \quad [2]$$

$$kC^{i}_{Se}(1 - \theta) = \frac{D_{Se}}{\Gamma}\frac{(C_{Se} - C^{i}_{Se})}{\delta} \quad [3]$$

$$\frac{i}{F} = D_{Ag}\frac{(C_{Ag} - C^{i}_{Ag})}{\delta} \quad [4]$$

Equations 1 and 2 are the mathematical expressions of the curvature enhanced accelerator coverage model.[4-9] Equation 1 details how the local silver deposition rate increases with the coverage of adsorbed catalyst, while Eq. 2 describes how the local coverage of adsorbed catalyst changes during metal deposition. More specifically, the Butler-Volmer equation, Eq. 1, expresses the local metal deposition rate as a function of the overpotential η, catalyst coverage θ, and the silver ion concentration at the interface C^{i}_{Ag} (for bulk concentration C_{Ag}). Evaluation of the coverage of the adsorbed catalyst is described by Eq. 2 where the first term describes local change of the catalyst coverage through local area change and the second term accounts for adsorption from the electrolyte according to Langmuir

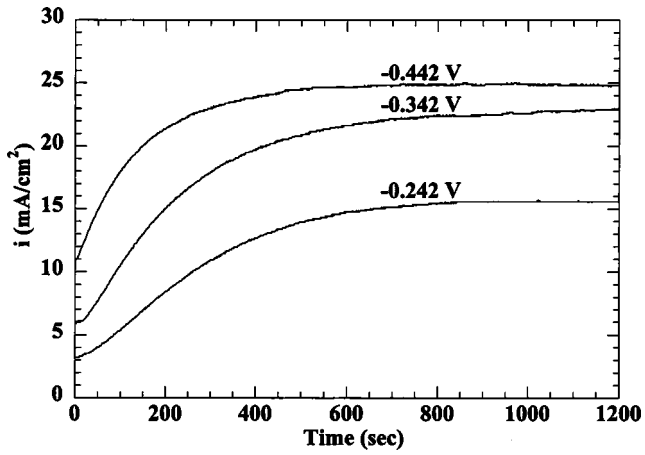

Figure 2. Current transient plots for 0.34 mol/L $KAg(CN)_2$, 2.3 mol/L KCN, and 1 μmol/L KSeCN for three overpotential values.

kinetics (for concentration C^{i}_{Se} at the interface). Note that the time rate of change of local area equals the normal velocity $v = i\Omega_{Ag}/F$, with $\Omega_{Ag} = 10.3$ cm^3/mol and Faraday's constant, $F = 96{,}485$ C/mol, multiplied by the local curvature κ. For planar substrates, such as were used in acquiring the i-η data, the curvature $\kappa = 0$.

For planar substrates, mass balance, assuming a psuedo-steady-state approximation, yields Eq. 3, which matches the flux of catalyst adsorbing on the surface with that diffusing across a boundary layer of thickness δ, for diffusion coefficient D_{Ag}. Likewise, Eq. 4 matches the rate of silver ion incorporation into the deposit with the flux of silver ions across the boundary layer.

The i-η data were fit as follows. First, the time-dependent coverage of selenium, $\theta(t,k)$, is obtained for a particular electrolyte concentration C_{Se} and rate constant k, by numerically integrating Eq. 2 for a −1 mV/s sweep rate. The time-dependent current is then obtained using Eq. 1, for particular functions $\alpha(\theta)$ and $i_o(\theta)$. The functions $\alpha(\theta)$ and $i_o(\theta)$, both presumed to be linear in θ, and the rate constant k were obtained by optimizing the fit to the experimental i-η curves obtained for the eleven different concentrations of KSeCN catalyst. Values used for Γ, the maximum possible coverage of adsorbed catalyst, and D_{Ag} in Eq. 1-3 were the same as those used in a previous publication[4]: 7.6×10^{-10} mol/cm^2 and 7.6×10^{-6} cm^2/s, respectively. The diffusion coefficient D_{Se} for the selenium catalyst was set equal to D_{Ag}. The bulk concentration of the catalyst $SeCN^-$ was assumed to be the known concentration of KSeCN; the bulk concentration of silver is assumed to be the same as the concentration of $KAg(CN)_2$. A voltage independent $k = 1.05 \times 10^6$ cm^3/mol s, with $F/RT = 38.92$ V^{-1} at $T = 293$ K and overpotential η in volts, was found to fit the data well. The resulting fits for the kinetic parameters are $i_o = 0.18 + 5.4\theta$ mA/cm^2 and $\alpha = 0.23 + 0.12\theta$. The boundary layer thickness δ was also used as a fitting parameter; a value of 95 μm optimized the fit. For these parameters, the limiting current associated with transport of the metal ions, equal to $D_{Ag}C_{Ag}F/\delta$, has a value of 26.2 mA/cm^2. The fits for the eleven curves, each one a hysteretic cycle containing inflection points on both the outgoing and return sweeps, have an average root mean square deviation of less than 0.8 mA/cm^2 using only seven fitting parameters. Several of the i-η data curves and the associated simulations are shown in Fig. 3.

These kinetic parameters can now be utilized in the CEAC model to predict superfilling behavior in vias. The same equations are used for modeling feature filling as were used for modeling the i-η results. The only differences are that (*i*) all kinetic parameters are now

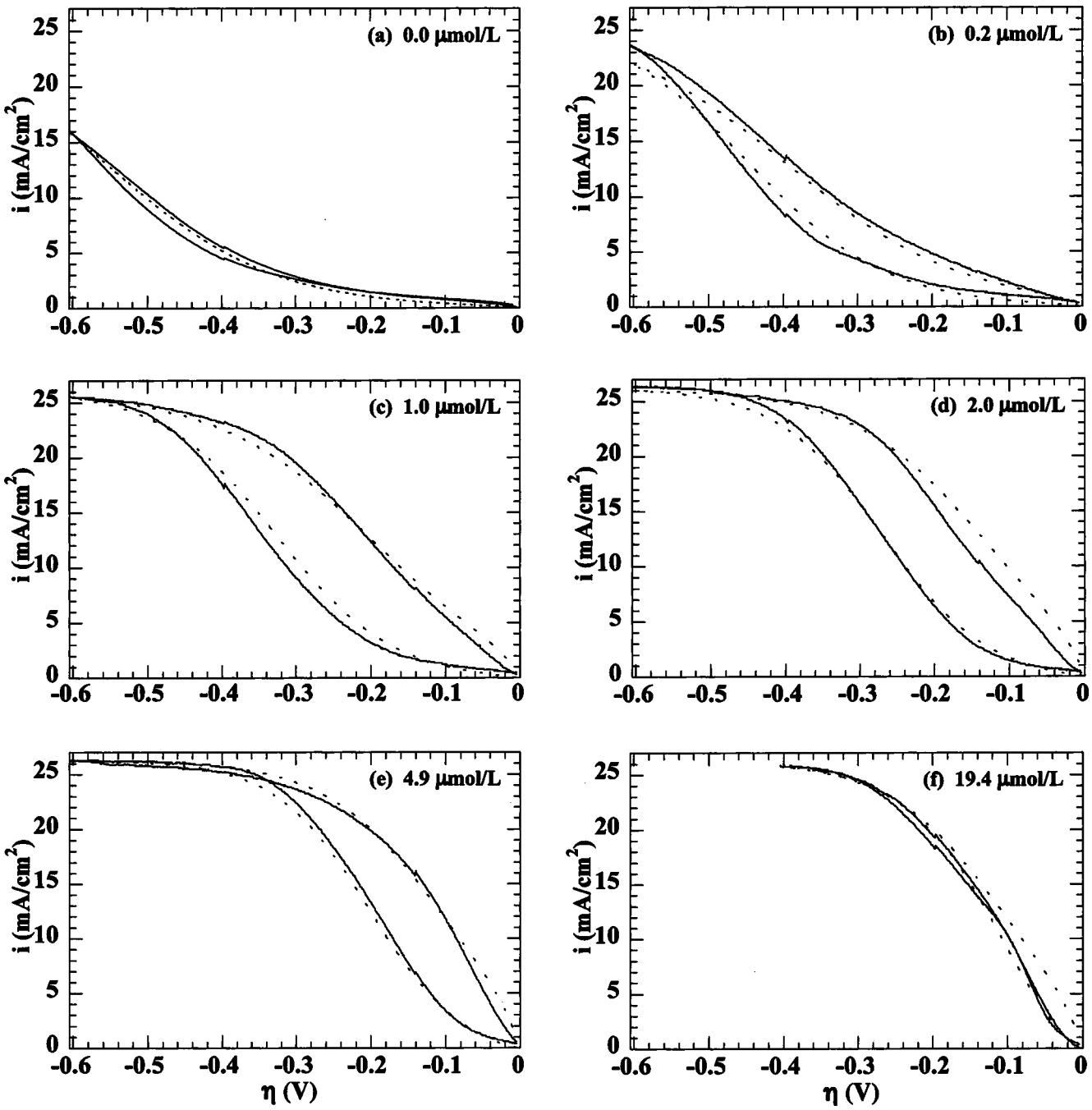

Figure 3. Comparison of experimental i-η curves (solid line) obtained on planar substrates with those obtained for the optimized kinetic parameters. Each plot differs only predicted (dashed line) in the concentration of KSeCN catalyst in the electrolyte. With the exception of the experimental results for the additive-free case, the outgoing sweeps are the curves with the lower current at a given voltage for both the experimental and modeling results. Both the bare surface (additive-free) and saturated surface (for 19.4 μmol/L KSeCN) behaviors are captured as is the time-dependent accumulation of the catalyst as manifested in the hysteresis loops at intermediate concentrations.

specified and (*ii*) the curvature κ of the surface is generally nonzero.

Modeling of Via Filling

A front tracking code, analogous to that previously used for modeling fill of trenches,[6] was used to model via filling. The code was appropriately modified to account for the cylindrical geometry of the via. Silver ion and catalyst depletion were approximated as that obtained for deposition on a planar substrate as per Eq. 3 and 4. Concentrations were assumed to be independent of position within the vias. All vias studied were 1.5 μm apart, nearly five times the largest via dimension, making additional metal ion or catalyst depletion due to deposition on the extra surface area (*i.e.*, the sidewalls) of the vias small enough to ignore. Time-dependent concentrations equal to those over a planar substrate for deposition under equivalent conditions (as per Eq. 3 and 4) were therefore used. Results are shown in Fig. 4 for electrolytes, deposition potentials and via aspect ratios chosen to match the experimental results. Aspect ratios were

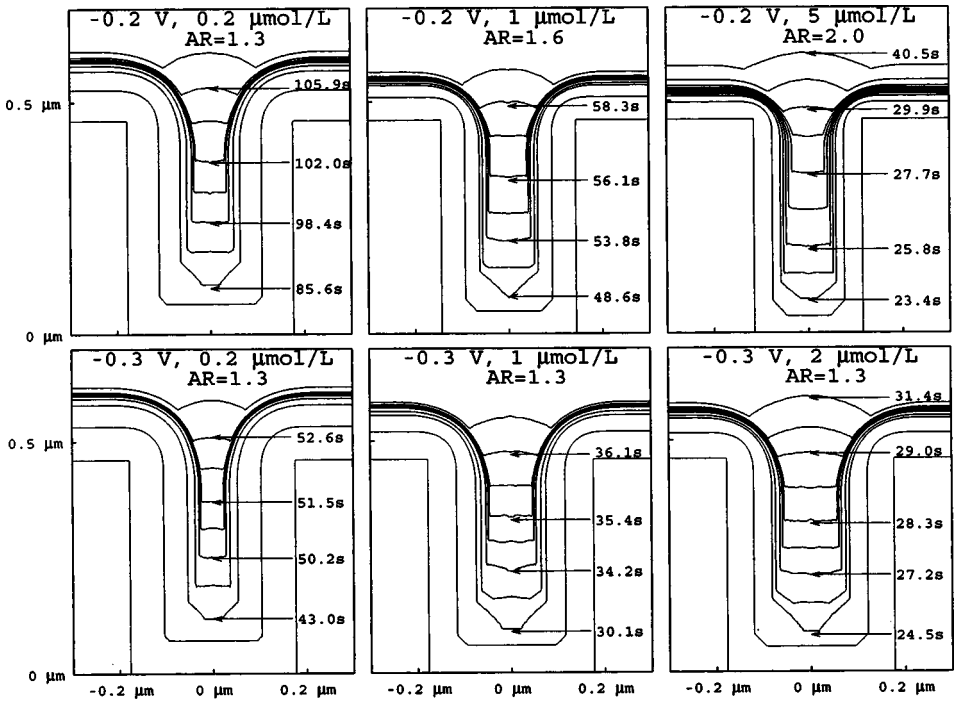

Figure 4. Filling predicted by the CEAC model. Simulations are shown for silver deposition in electrolytes containing 0.34 mol/L $KAg(CN)_2$, 2.3 mol/L KCN with different KSeCN concentrations and via aspect ratios indicated. Results for overpotential −0.2 V are shown on top and for −0.3 V on the bottom. Superconformal filling is predicted in all cases, as indicated by the bottom-to-top filling.

chosen to match those obtained using the experimental via heights divided by their diameters at midheight. Predictions based on the kinetics obtained from the i-η studies on planar substrates and the evolution Eq. 1 through 3 are shown in Fig. 4.

Deposition on patterned substrates.—Filling of vias with an aspect ratio of 1.3 (defined as above) in electrolytes at a deposition potential of −0.2 V and varying concentration of catalyst is shown in Fig. 5. The absence of voids in the via filled in 0.2 μmol/L KSeCN is consistent with superconformal filling (Fig. 5, top). The time sequence for deposition in 1 μmol/L KSeCN shows the bottom-to-top filling that is an unambiguous sign of superconformal deposition (Fig. 5, middle). A further increase of the catalyst concentration to 5 μmol/L KSeCN yields improved superconformal filling (based on the reduced thickness of the deposits on the sidewalls) at an aspect ratio (AR) of 2.0 (Fig. 5, bottom).

Filling of vias at a deposition potential of −0.3 V and varying concentrations of catalyst is shown in Fig. 6. In contrast to the results obtained at −0.2 V (Fig. 5), a void in the feature, and a cusp over it, both clear signs of conformal filling, are evident in the via filled in the electrolyte with 0.2 μmol/L KSeCN (Fig. 6, top). A time sequence at 1 μmol/L KSeCN shows the evolution of such failure (Fig. 6, middle). However, for a concentration of 2 μmol/L KSeCN, filling is clearly consistent with bottom-to-top superconformal filling (Fig. 6, bottom). The off-center void most likely formed as the upward moving bottom surface went across that location on the sidewall deposit.

Consistent with the experimental results at −0.2 V (Fig. 5), superconformal filling was predicted for the via of AR 1.3 via in 0.2 μmol/L KSeCN, AR 1.6 via in 1 μmol/L KSeCN and the AR 2.0 via in 5 μmol/L KSeCN (Fig. 4, top row). The sidewall thickness and height of the bottom surface are also generally consistent with the predicted times. In contrast, while the experimental results for filling of AR 1.3 vias at −0.3 V showed superconformal filling only for a catalyst concentrations of 2 μmol/L (Fig. 6, bottom), superconformal filling was predicted for 0.2, 1, and 2 μmol/L concentrations (Fig. 4, bottom row).

In light of the rapid motion of the bottom surface during the period of superconformal filling, agreement between predictions and experiment is excellent for filling in 5 μmol/L at −0.2 V and in 2 μmol/L at −0.3 V. The source of the disagreement between model

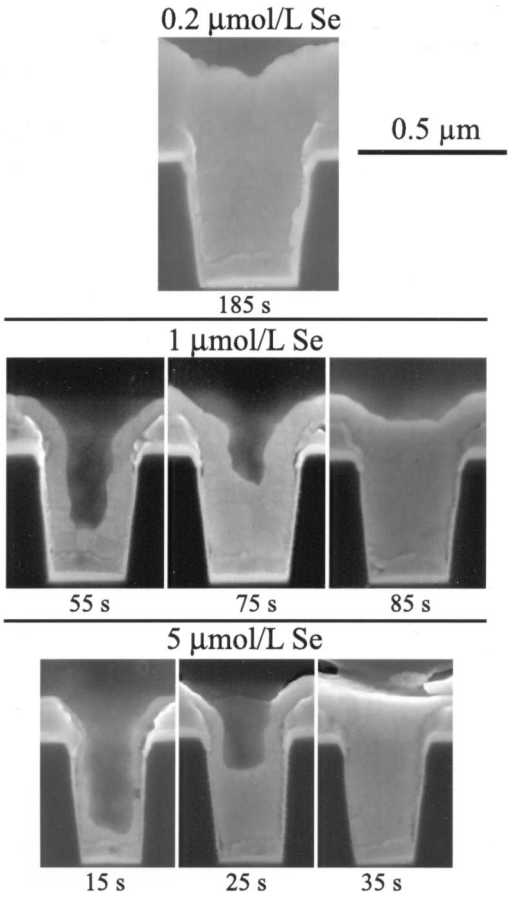

Figure 5. Silver filling of vias at an overpotential of −0.2 V in electrolytes containing 0.34 mol/L $KAg(CN)_2$, 2.3 mol/L KCN, and (top) AR 1.3 for 0.2 μmol/L KSeCN, (middle) AR 1.6 for 1 μmol/L KSeCN, and (bottom) AR 2.0 for 5 μmol/L KSeCN. The absence of a void for 0.2 μmol/L KSeCN is consistent with the evident superconformal filling for the 1 μmol/L KSeCN and the 5 μmol/L KSeCN.

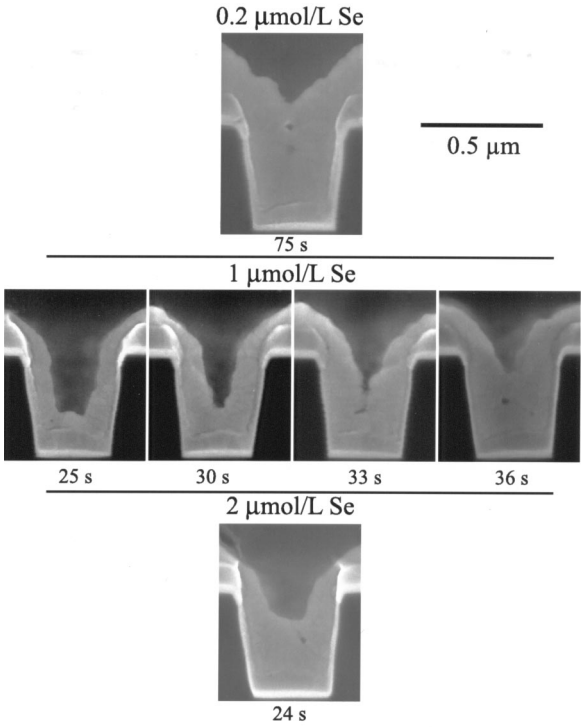

Figure 6. Silver filling of vias at an overpotential of −0.3 V in electrolytes containing 0.34 mol/L $KAg(CN)_2$, 2.3 mol/L KCN, and (top) 0.2 μmol/L KSeCN, (middle) 1 μmol/L KSeCN, and (bottom) 2 μmol/L KSeCN. The central void and cusped surface for 0.2 μmol/L KSeCN are consistent with conformal filling as shown for the 1 μmol/L KSeCN. Superconformal bottom-to-top filling is evident for the 2 μmol/L KSeCN in spite of the off-center void.

and experiment for the 0.2 and 1 μmol/L catalyst concentrations at −0.3 V is unclear, although one possibility is surface roughness. Note particularly the roughness of the sidewall deposits for the experimental results that the model failed to predict accurately (Fig. 6, top and middle). Surface roughness has previously been noted to lead to void formation where it is not otherwise expected.[4]

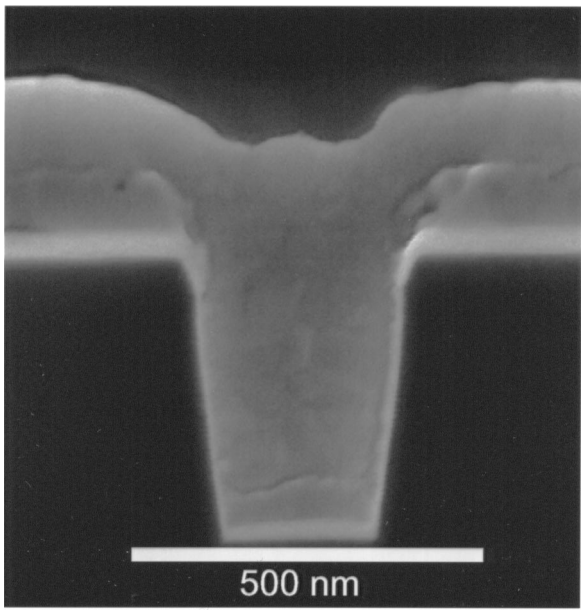

Figure 7. An overfill bump is visible above the fully filled via. Silver deposition was accomplished in an electrolyte containing 0.34 mol/L $KAg(CN)_2$, 2.3 mol/L KCN, and 1 μmol/L KSeCN at an overpotential of −0.2 V for 85 s.

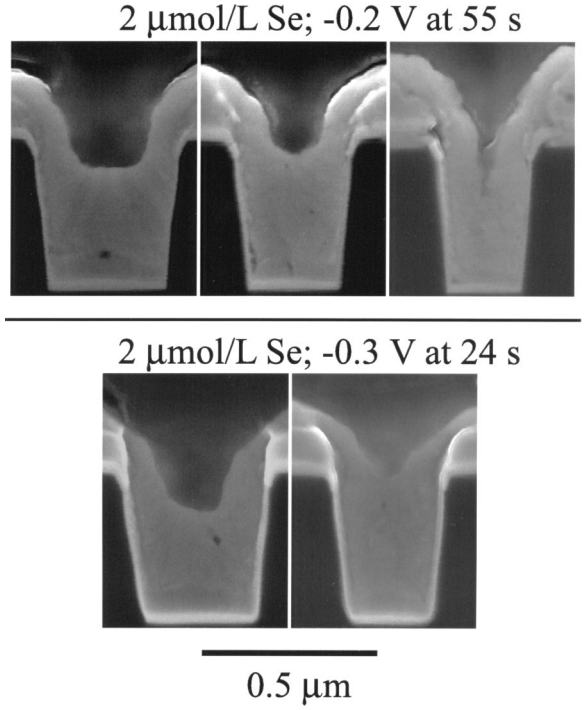

Figure 8. Silver fill of vias in electrolytes containing 0.34 mol/L $KAg(CN)_2$, 2.3 mol/L KCN, and 2 μmol/L KSeCN at (top) −0.2 V and (bottom) −0.3 V. The sidewall thicknesses on the vias that have nearly finished bottom-to-top filling permit the maximum aspect ratios for superconformal filling to be estimated.

Once bottom-to-top superconformal filling of the feature is finished, a bump develops over the feature (Fig. 7). This is in agreement with model predictions shown in Fig. 4, and with previous experimental and modeling predictions for superconformal copper deposition.[5-9] As per the model predictions, the rapid upward motion of the bottom surface is due to the increased catalyst coverage there induced through area decrease during deposition on the concave surface. The resulting increased catalyst coverage causes enhanced deposition on this surface even after it leaves the via, creating the bump visible above the fully filled feature. The overfill bump is thus a direct result of the same CEAC mechanism that is responsible for the superconformal bottom-to-top filling of the feature itself. Note that, due to the opposite sign curvature of the surface, which becomes convex after leaving the via, deposition on the bump deaccelerates toward that on the planar surface with further deposition.

Estimating the limits.—It is possible to estimate the maximum aspect ratio feature that can be filled using superconformal filling results on a lower aspect ratio feature. This maximum value is the feature height divided by the twice the sidewall thickness just prior to completion of filling. While this construct is strictly accurate for filling of trenches, it is only approximate for filling of vias because the fractional decrease of sidewall area for a given thickness of deposit scales inverselt with the radius. This makes estimates of the maximum fillable aspect ratio based on larger diameter vias liberal. As an example, a sidewall thickness of ≈0.1 μm just prior to filling of the two larger diameter vias in 2 μmol/L KSeCN at −0.2 V (Fig. 8, top) yields a minimum via diameter of ≈0.2 μm for superconformal filling. Using the via height of 0.46 μm, this indicates that AR 2.3 is the highest that can be filled for these conditions. This is reasonably consistent with the failure of the AR 2 via for these conditions. Similarly, the sidewall thickness of ≈0.125 μm just prior to via filling of the larger diameter via in 2 μmol/L KSeCN at −0.3 V

(Fig. 8, bottom) yields a minimum diameter of ≈0.25 μm and a maximum AR 1.8 for the same electrolyte at −0.3 V. Again, this is reasonably consistent with the marginal failure observed in the 1.7 AR feature for these conditions. Based on the ≈0.05 μm thick sidewalls for the via filled for 25 s in 5 μmol/L KSeCN at −0.2 V (see Fig. 5, bottom), a minimum diameter of ≈0.1 μm and a maximum AR 4.6 are obtained.

Conclusion

This work has presented an electrolyte containing a single Se-based additive that yields superconformal silver electrodeposition in fine features. The curvature enhanced accelerator coverage (CEAC) model, using kinetics obtained from deposition behavior on planar substrates, was used to quantitatively predict the filling behavior.

The National Institute of Standards and Technology assisted in meeting the publication costs of this article.

References

1. R. Manepalli, F. Stepniak, S. A. Bidsturp-Allen, and P. A. Kohl, *IEEE Trans. Adv. Packag.*, **22**, 4 (1999).
2. M. Hauder, W. Hansch, J. Gstöttner, and D. Schmitt-Landsiedel, *Microelectron. Eng.*, **60**, 51 (2002).
3. T. L. Alford, Y. Zeng, P. Nguyen, L. Chen, and J. W. Mayer, *Microelectron. Eng.*, **55**, 389 (2001).
4. T. P. Moffat, B. Baker, D. Wheeler, J. E. Bonevich, M. Edelstein, D. R. Kelly, L. Gan, G. R. Stafford, P. J. Chen, W. F. Egelhoff, and D. Josell, *J. Electrochem. Soc.*, **149**, C423 (2002).
5. D. Josell, B. Baker, C. Witt, D. Wheeler, and T. P. Moffat, *J. Electrochem. Soc.*, **149**, C637 (2002).
6. T. P. Moffat, D. Wheeler, W. H. Huber, and D. Josell, *Electrochem. Solid-State Lett.*, **4**, C26 (2001).
7. D. Josell, D. Wheeler, W. H. Huber, and T. P. Moffat, *Phys. Rev. Lett.*, **87**, 016102 (2001).
8. D. Josell, D. Wheeler, W. H. Huber, J. E. Bonevich, and T. P. Moffat, *J. Electrochem. Soc.*, **148**, C767 (2001).
9. D. Josell, D. Wheeler, and T. P. Moffat, *Electrochem. Solid-State Lett.*, **5**, C44 (2002).
10. M. Ota, M. Tsujimura, H. Inoue, H. Ezawa, and M. Miyata, in *Proceedings of the Spring Meeting of the Materials Research Society*, San Francisco, CA (April 2002), Pending.